Journal of Alloys and Compounds 505 (2010) 324–327

Contents lists available at ScienceDirect

Journal of Alloys and Compounds

journal homepage: www.elsevier.com/locate/jallcom

CdS semiconductor nanoparticles embedded in AlMCM-41 by solid-state reaction

Sh. Sohrabnezhad [a,*], A. Pourahmad [b]

[a] Department of Chemistry, Faculty of Science, University of Mohaghegh Ardabili, Ardabil, Iran
[b] Department of Chemistry, Faculty of Science, Islamic Azad University, Rasht Branch, Rasht, Iran

ARTICLE INFO

Article history:
Received 19 January 2010
Received in revised form 4 June 2010
Accepted 10 June 2010
Available online 17 June 2010

Keywords:
CdS nanoparticles
AlMCM-41
Nanocomposites
Solid-state reaction
XRD

ABSTRACT

Nanoparticles (NPs) of CdS encapsulated in AlMCM-41 were prepared by a novel technique with non-aqueous systems. The mechanical mixture of $CdCl_2$ crystal with AlMCM-41 was heated at 773 K, followed by the H_2S treatment at 373 K, resulting in the formation of Cadmium sulphide NPs with the size of 2 nm. The final product (CdSAlMCM-41) was characterized by X-ray diffraction (XRD) pattern, transmission electron microscopy (TEM), scanning electron microscopy (SEM) and UV–vis spectroscopy.

1. Introduction

Semiconductor nanoparticles have been extensively investigated during the last decade, due to their unique properties and application potential in diverse areas such as photocatalysis, solar cells, display panels and new devices like single electron transistors and so on [1–6]. Many nanostructured prototypes have been obtained using different experimental procedures looking for enhanced physical properties related to (a) homogeneity, (b) stability to different environmental factors, (c) reproducibility and (d) scaling at the industrial level of those structures. Nevertheless, many of these requirements have not already been solved, especially those oriented to opto-electronic applications. Traditionally, colloidal solutions [7], porous glasses [8] and certain polymers [9] have been used as hosts for the preparation of nanosized materials. However, they are neither efficient in generating clusters of uniform size nor chemically inert towards the guest molecules. On the other hand, it was realized that the preparation of nanosized materials in zeolitic pores has several advantages and hence they have been considered to form ideal host systems [10,11]. Indeed, the regular pore structure of zeolite molecular sieves offers a suitable reaction chamber for the controlled assembling of nanostructured materials [12–15]. However, the smaller pore size of these materials limits their applicability. On the other hand, the recent discovery of mesoporous molecular sieves designated as M41S [16] have broadened the scope of applications. Two of the stable members of the M41S family, viz., hexagonal MCM-41 having unidimensional pore structure and cubic MCM-48 with three-dimensional pore system can comfortably trap the guest molecules in the mesopores [17–20]. Further, the well-defined pore size, large internal surface area associated with the open framework of the mesophases show promise for such purpose. Therefore, in the present investigation AlMCM-41 was used as host material, and CdS was selected as the guest molecule. Moreover, we wish to report a novel technique of synthesizing semiconductor NPs encapsulated in AlMCM-41.

2. Experimental

The MCM-41 and AlMCM-41 materials were synthesized by a room temperature method with some modification in the described procedure in the literature [21]. We used tetraethylorthosilicate (TEOS, Merck, 800,658) as a source of silicon and hexadecyltrimethylammonium bromide (HDTMABr, BDH, 103,912) as a surfactant template for preparation of the mesoporous materials. The molar composition of the reacting mixture was as follows:

$$SiO_2 : 1.6EA : 0.215HDTMABr : 325H_2O$$

EA stands for ethylamine. The MCM-41 prepared was calcined at 550 °C for 5 h to decompose the surfactant and obtain the white powder. This powder was used as the parent material to prepared AlMCM-41 free surfactant materials by post-synthesis alumination method. The AlMCM-41surfactant-free material is white. This powder sample was used for loading the nanoparticles.

The syntheses of CdS NPs in AlMCM-41 were carried out by the following method. AlMCM-41 was mixed mechanically with $CdCl_2$ crystal. The resulting mixture was heated at 773 K for 4 h in air, and then exposed to H_2S at 373 K for 1 h. The CdS particles prepared from AlMCM-41 are described as CdSAlMCM-41, in subsequent discussions.

For the sake of comparison, bulk CdS particles were prepared by a conventional precipitation method. In this method, an equimolar amount of Na_2S solution was added dropwise to a stirred solution of 1 M $CdCl_2$ resulting in the formation of CdS precipitates. The CdS precipitate was washed repeatedly with distilled water until

---

* Corresponding author. Tel.: +98 451 2234432; fax: +98 451 5514024.
E-mail address: sohrabnezhad@uma.ac.ir (Sh. Sohrabnezhad).

0925-8388/$ – see front matter © 2010 Published by Elsevier B.V.
doi:10.1016/j.jallcom.2010.06.065

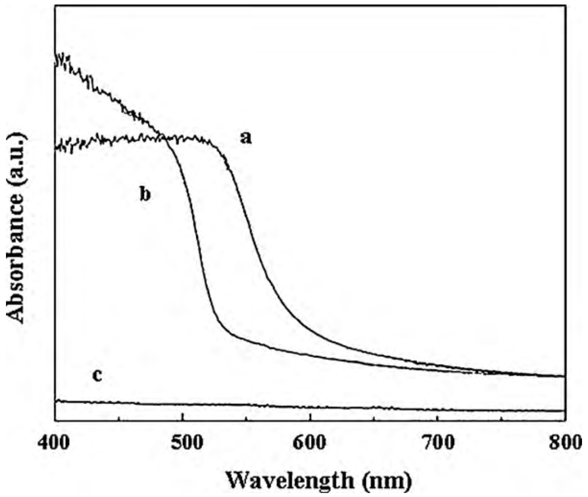

Fig. 1. UV–vis absorption spectrum of (a) bulk CdS, (b) CdSAlMCM-41 and (c) AlMCM-41.

free from S^{2-} ions, dried in an air-oven and then calcined at 400 °C for 4 h in air.

Powder X-ray diffraction patterns of the samples were recorded using a Philips X, Pert diffractometer with Cu K_α radiation ($\lambda = 1.54$ Å). UV–vis absorption spectra were recorded using a Shimadzu 1600 PC in the spectral range of 190–900 nm. The specific surface area and pore volume of the samples were measured using a Sibata Surface Area Apparatus 1100. All of the samples were first degassed at 250 °C for 2 h. The amount of constituent elements in samples was examined with inductively coupled plasma-optical emission spectrometry (ICP-OES), Perkin-Elmer OPTIMA-3000. The surface morphology of the samples was obtained using a Jeol-JSM-5610 LV scanning electron microscopy (SEM). The transmission electron micrographs (TEM) were recorded with a Philips EM208 microscope, working at a 100 kV accelerating voltage. Samples for TEM were prepared by dispersing the powdered sample in acetone by sonication and then drip drying on a copper grid (400 mesh) coated with carbon film. Temperature programmed desorption measurement was carried out for the mechanical mixture of $CdCl_2$ with zeolite, where the effluent gas was monitored with an Anelva AQA-200 mass spectrometer.

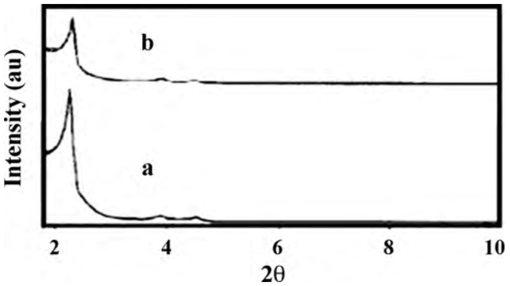

Fig. 2. X-ray diffraction patterns of (a) AlMCM-41 and (b) CdAlMCM-41 or CdSAlMCM-41.

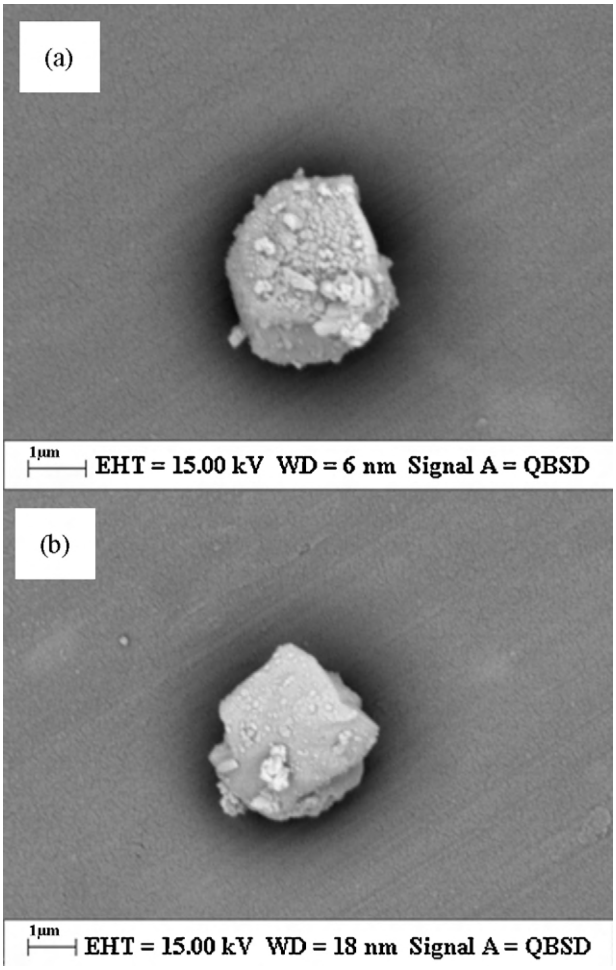

Fig. 3. Scanning electron microscopy (SEM) micrographs of (a) AlMCM-41 and (b) CdSAlMCM-41.

3. Results and discussion

UV–vis absorption spectra for CdS NPs prepared from AlMCM-41 matrices, bulk CdS, and AlMCM-41 are shown in Fig. 1. The parent AlMCM-41 (Fig. 1c) gave no absorption in the range 400–800 nm, while the bulk CdS (Fig. 1a) gave a wide absorption below 600 nm. Comparing the absorption edge of bulk CdS to that of CdSAlMCM-41 sample prepared from mesoporous materials, it is seen that a blue shift in the onset of absorption is observed in this sample. This blue shift indicates that CdS exists as small clusters within the zeolite pores as reported by several researchers [22,23]. This was supported by a significant decrease in the surface area of CdSAlMCM-41, compared to the parent zeolite (Table 1). This phenomenon of blue shift of absorption edge has been ascribed to a decrease in particle size. It is well known that in case of semiconductors the band gap between the valence and conduction band increases as the size of the particle decreases in the nanosize range. This results in a shift in the absorption edge to a lower wavelength region. The magnitude of the shift depends on the particle size of the semiconductor. In the present study, the CdSAlMCM-41 samples prepared from the AlMCM-41 matrix showed a blue shift of approximately 75 nm compared to the bulk particles. From the onset of the absorption edge, the band gap of the CdS particles was calculated using the method of Tandon and Gupta [24] (Table 1). The size of

Table 1
Specific surface area[a], pore volume[a], band gap[b], particle size[b] and Cd/Al ratio[c] of samples.

Samples	Specific surface area ($m^2\,g^{-1}$)	Pore volume ($cm^3\,g^{-1}$)	Band gap (eV)	Particle size (nm)	Cd/Al ratio
AlMCM-41	949	0.9	–	–	–
CdSAlMCM-41	556	0.4	3.51	2	0.43
Bulk CdS	15	0.053	2.03	16	–

[a] Determinated by BET method.
[b] See in the text.
[c] Determinated by ICP method.

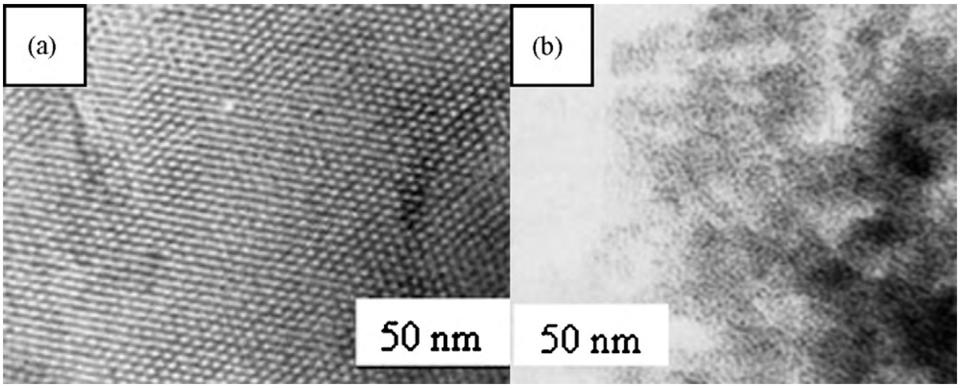

Fig. 4. Transmission electron microscopy (TEM) images of (a) AlMCM-41 and (b) CdSAlMCM-41.

CdS NPs, estimated based on the results of Weller et al. [25], was 2 nm for CdSAlMCM-41 sample.

Fig. 2 shows the XRD patterns of the samples. Measurements of the samples were carried out in the 2θ different ranges (2θ = 2–10° and 2θ = 0–80°), under the conditions of 40 kV and 40 mA, at a step size of 2θ = 0.02°. The AlMCM-41 support exhibited only a broad (1 0 0) peak at 2θ = 2.5°, while other diffraction peaks corresponding to the (1 1 0) and (2 0 0) crystal plans were unresolved due to the large amount of aluminum incorporation [26,27]. In this figure, we observed that all X-ray patterns are very similar. But, some differences, such as the broadening and slight shifting to higher angles of the diffraction peaks as well as the decrease of their intensity can be observed in the spectra. This should be attributed to the pore-filling effects that can reduce the scattering contrast between the pores and the framework AlMCM-41 materials. These decreases of the peak intensities are in agreement with the reported results for other zeolites [28–30]. On the other hand, it is of interest to note that the characteristic peaks assigned to $CdCl_2$ disappeared completely. Since no change in the amount of Cd was confirmed by ICP method for the sample before and after calcination at 773 K for 4 h, the disappearance of the XRD peaks of $CdCl_2$ crystal might be explained by the high dispersion of $CdCl_2$ in the pores of AlMCM-41 or the change to amorphous phase from crystal phase. The former explanation is more appropriate because a similar phenomenon that the CuCl highly dispersed by heat-treatment in the channel of Na-ZSM-5 has been reported [31]. On exposing the sample to H_2S, no new diffraction peak was detected in the range 2θ = 2–10° and 2θ = 0–80°, as shown in Fig. 2b.

The mass spectra of effluent gases during the heat-treatment were recorded for AlMCM-41 + $CdCl_2$. The sample of the mechanical mixture of $CdCl_2$ with AlMCM-41 gave the peak of effluent H_2O below 500 K. It was found that the former peak came from both the desorption of H_2O adsorbed on AlMCM-41 and the dehydration of $CdCl_2$, compared to the references, AlMCM-41 and $CdCl_2$.

On the basis of the results of XRD and mass spectra, the reaction scheme during heat-treatment will be discussed. The reaction scheme of the mechanical mixture of $CdCl_2$ with AlMCM-41 is not clear; however, it is expected that the following reaction takes place for the mechanical mixture of $CdCl_2$ with AlMCM-41 during the heat treatment:

$$\underset{(\mathrm{m,AlMCM-41\ mesopore})}{2\mathrm{Na}^+ + \mathrm{CdCl}_2} \rightarrow \mathrm{Cd}^{2+} + 2\mathrm{NaCl}$$

The above reaction indicates that divalent cadmium ion was ion-exchanged with two Na^+ ions even in a solid state. A similar solid-state ion-exchange was reported by Karge and Beyer [32,33].

The results of the specific surface area and pore volume measurements (BET measurements) for AlMCM-41, CdSAlMCM-41, and bulk CdS, show that the pore volumes of the host mesoporous material, which was 0.9 ml g^{-1} for AlMCM-41, decreased to 0.4 ml g^{-1} for CdSAlMCM-41 materials. Similarly, the specific surface areas of the composite materials were decreased from 949 m^2 g^{-1} for AlMCM-41 to 556 m^2 g^{-1} for CdSAlMCM-41. Decreasing of the volumes of the pores and the specific surface area of the mesoporous material demonstrates that the guests are located in the channels (Table 1).

The surface morphology of AlMCM-41 and CdSAlMCM-41 is investigated by SEM and the micrographs are presented in Fig. 3. It can be seen that the crystallites of the unloaded mesoporous material, with size between 1 and 2 μm, have a well-defined shape (Fig. 3a). There is no considerable change in morphology of CdSAlMCM-41.

Transmission electron microscopy along with the textural properties of the samples discussed above bring us important information regarding whether the CdS particles are located inside or outside the pore structures used in this work. TEM images of AlMCM-41 and CdSAlMCM-41 samples are shown in Fig. 4a and b, respectively. They were recorded under the direction parallel to the pore axis and it is possible to observe the typical AlMCM-41 morphology in both micrographs. Although it is very difficult to identify CdS NPs within the pores of MCM-41 materials using TEM techniques [34], the higher contrast in the image of the CdSAlMCM-41 sample can be associated with the presence of CdS nanocrystals inside the pores of this sample.

4. Conclusions

In this study, we have reported a novel and simple method to synthesize CdS nanoparticles in AlMCM-41 material hosts. A blue shift in the absorption edge was observed in the samples prepared by a solid-state reaction method, indicating the formation of nanometer-sized CdS NPs in AlMCM-41 mesopore, as a consequence of particle size effects.

Acknowledgment

We thank Miss. Arezoo Pourahmad for her aids.

References

[1] H.-F. Yu, S.-T. Yang, J. Alloys Compd. 492 (1–2) (2010) 695.
[2] C.E. Rodríguez-Torres, S.J. Stewart, C. Adán, A.F. Cabrera, J. Alloys Compd. 495 (2) (2010) 485.
[3] H.-J. Bai, Z.-M. Zhang, Mater. Lett. 63 (2009) 764–766.
[4] J. Wu, X. Lü, L. Zhang, Y. Xia, F. Huang, F. Xu, J. Alloys Compd. 496 (1–2) (2010) 234.
[5] G. Mandal, S. Bhattacharya, T. Ganguly, Chem. Phys. Lett. 478 (2009) 271.
[6] P.K. Sharma, R.K. Dutta, A.C. Pandey, J. Colloid Interface Sci. 345 (2010) 149.
[7] V.S. Lebedev, A.G. Vitukhnovsky, A. Yoshida, N. Kometani, Y. Yonezawa, Colloids Surf. A 326 (3) (2008) 204.
[8] R.W. Gerber, D.N. Leonard, S. Franzen, Thin Solid Films 517 (24) (2009) 6803.

[9] B. Sadeghi, M.A.S. Sadjadi, R.A.R. Vahdati, Superlattices Microstruct. 46 (6) (2009) 858.
[10] A. Pourahmad, Sh. Sohrabnezhad, E. Radaee, J. Porous Mater. 17 (3) (2010) 367.
[11] C.J. Van Oers, W.J.J. Stevens, E. Bruijn, M. Mertens, O.I. Lebedev, G. Van Tendeloo, V. Meynen, P. Cool, Micropor. Mesopor. Mater. 120 (1–2) (2009) 29.
[12] H.R. Emamian, A. Honarbakhsh-raouf, A. Ataie, A. Yourdkhani, J. Alloys Compd. 480 (2) (2009) 681.
[13] A. Pourahmad, Sh. Sohrabnezhad, J. Alloys Compd. 484 (2009) 314.
[14] A. Pourahmad, Sh. Sohrabnezhad, M.S. Sadjadi, K. Zare, Mater. Lett. 62 (2008) 655.
[15] Sh. Sohrabnezhad, A. Pourahmad, M.A. Zanjanchi, J. Iran. Chem. Soc. 6 (3) (2009) 612.
[16] C.T. Kresge, M.E. Leonowicz, W.T. Roth, J.C. Vartuli, J.S. Beck, Nature 359 (1992) 710.
[17] E. Caponetti, L. Pedone, M.L. Saladino, D. Chillura Martino, G. Nasillo, Micropor. Mesopor. Mater. 128 (2010) 101–107.
[18] Sh. Sohrabnezhad, A. Pourahmad, E. Radaee, J. Hazard. Mater. 170 (2009) 184.
[19] A. Popa, V. Sasca, J. Halasz, Appl. Surf. Sci. 255 (2008) 1830–1835.
[20] S. Chaliha, K.G. Bhattacharyya, Catal. Today 141 (2009) 225–233.
[21] A.C. Voegtlin, A. Matijasic, J. Patarin, C. Saucrland, Y. Griller, L. Huve, Micropor. Mater. 10 (1997) 137.
[22] Y. Wang, N. Herron, J. Phys. Chem. 91 (1987) 257.
[23] W. Chen, Z. Wang, L. Lin, J. Lumin. 71 (1997) 151.
[24] S.P. Tandon, J.P. Gupta, Phys. Status Solidi 38 (1970) 363.
[25] T. Vossmeyer, L. Katsikas, M. Giersig, I.G. Popovic, K. Diesner, A. Chemseddine, A. Eychmuller, H. Weller, J. Phys. Chem. 98 (1994) 7665.
[26] K. Chaudhari, T.K. Das, A.J. Chandwadkar, S. Sivasaker, J. Catal. 186 (1999) 81.
[27] S. Biz, J. Phys. Chem. B 103 (1999) 8432.
[28] M. Flores-Acosta, M. Sotelo-Lerma, H. Arizpe-Charez, F.F. Castillon-Barraza, R. Ramirez-Bon, Solid State Commun. 128 (2003) 407.
[29] R. Ochoa-Landin, M. Flores-Acosta, R. Ramirez-Bon, H. Arizpe-Charez, M. Sotelo-lerma, F.F. Castillon-Barraza, J. Phys. Chem. Sol. 64 (2003) 2245.
[30] M. Sathish, B. Viswanathan, R.P. Viswanathan, Int. J. Hydrogen 31 (2006) 891.
[31] G. Spoto, A. Zecchina, S. Bordiga, G. Ricchiardi, G. Marta, G. Leofanti, G. Petrini, Appl. Catal. B 3 (1994) 151.
[32] H.G. Karge, H.K. Beyer, Stud. Surf. Sci. Catal. 69 (1991) 43.
[33] H.G. Karge, in: E. Derouane, C. Naccache, F.R. Ribeiro (Eds.), Zeolite Microporous Solids: Synthesis Structure, and Reactivity, Kluwer Academic Publisher, Dordrecht, The Netherlands, 1992, p. 273.
[34] H. Wellmann, J. Rathousky, M. Wark, A. Zukal, G. Schulz-Ekloff, Micropor. Mesopor. Mater. 44 (2001) 419.